Global mode visualisation in cavitating flows

[1]James A. Venning*; [1]Dean R. Giosio; [1]Bryce W. Pearce; [1]Paul A. Brandner

[1]*Cavitation Research Laboratory, University of Tasmania, Launceston, Tasmania, Australia*

Abstract

A technique for visualising global frequency modes and phasing information is presented using fast Fourier transforms applied to individual pixel intensities of high-speed photography image frames. A singular value decomposition is applied to the resulting complex data set to allow the application of windowing to the transforms. A high-speed image set of cloud cavitation about a sphere is used to demonstrate the technique and identify the dominant cavitation shedding modes. Three frequencies were found and the modal analysis show these to correspond to large-scale near symmetric shedding, intermediate-scale oblique shedding, and small-scale near symmetric shedding, respectively. Results obtained by the presented image analysis technique show close agreement to shedding frequencies obtained from pressure data.

Keywords: modal decomposition; mode visualisation; cavitation; high-speed imaging; frequency analysis

Introduction

Modal decomposition methods have been used in a variety of fluid mechanics applications to approximately describe complicated physical phenomena with few dimensions. Two commonly used techniques are the proper orthogonal decomposition (POD) and the dynamic mode decomposition (DMD). The POD ranks spatial structures according to the kinetic energy, if the data set is velocities [1]. This allows filtering based on energy so that experimental noise and turbulence can be removed. The DMD is based on growth-rates of frequencies, so that amplifying or decaying features can be extracted, but permanent features are not accentuated [e.g. 2, 3].

Here we present a technique based on the fast Fourier transform (FFT) of the pixel intensity in high-speed images. The objectives are to identify dominant frequencies in the videos, identify the regions in the spatial domain where these modes are manifested and to identify the phasing differences across the domain. This technique has been used previously in Basley et al. [4, 5] and [6], but here we extend the technique to enable the 'averaging' of multiple time instances to remove noise from the modes, as introduced by Venning [7] for velocimetry data.

In order to demonstrate the features of the decomposition, an example flow of cavitation about a sphere at a Reynolds number of $Re = U_\infty D/\nu = 1.5\times10^6$ and a cavitation number $\sigma = 2(p_\infty - p_v)/\rho U_\infty^2 = 0.8$ is presented. The sphere was sting-mounted in the centre of the tunnel test-section and the cavity was visualised with a Photron SA-5 high-speed camera acquiring megapixel images at 7000 fps. The conditions here match that of [8], and the three frequencies extracted from our video analysis correspond to those from the pressure measurements. The nature of the shedding modes of the cloud cavities are able to be distinguished using the decomposition here.

Spectral density estimation

The fast Fourier transform (FFT) is applied to the pixel intensity time series at each pixel location on the image. A Welch periodogram with Hanning windows was used to estimate the spectral density. For each data set, the window length, N, was 8192 points, representing 1.2 s or approximately 30 cycles of the dominant frequency, though this frequency was estimated as it varies with the cavitation number. The shift between windows, N_S, was 256 points. Given the time sequence is 21,000 points, there were $T = 51$ windows.

For each position (j) in the image plane, and each Welch window (t), the FFT of the pixel's intensity signal (x_n) is given by equation 1 with P and ϕ corresponding to the power and phase of each sinusoidal component of the time series, while f is the wavenumber. $\mathrm{Arg}(X_{jtf})$ returns the principal value of the angle from the real axis to a line from the origin to the complex number X_{jtf}, which in a practical sense, is $\mathrm{atan2}(\mathrm{Im}(X_{jtf}), \mathrm{Re}(X_{jtf}))$.

*Corresponding Author, James Venning: mail@jamesvenning.net

$$
\begin{aligned}
X_{jtf} &= \mathscr{F}(x_{jtf}) = \sum_{n=0}^{N-1} x_n \cdot e^{-2\pi i f n/N} \\
P_{jtf} &= \sqrt{\mathrm{Re}(X_{jtf})^2 + \mathrm{Im}(X_{jtf})^2} \\
\phi_{jtf} &= \mathrm{Arg}(X_{jtf})
\end{aligned}
\tag{1}
$$

The averaging across the T windows is trivial for the power (equation 2). For the case of the sphere, the average of the spectra across the spatial domain, $\langle \overline{P_{jf}} \rangle_j$ (figure 1) finds three key frequencies, as was reported in de Graaf et al. [8].

$$
\overline{P_{jf}} = \frac{1}{T} \sum_{t=1}^{T} P_{jtf} \tag{2}
$$

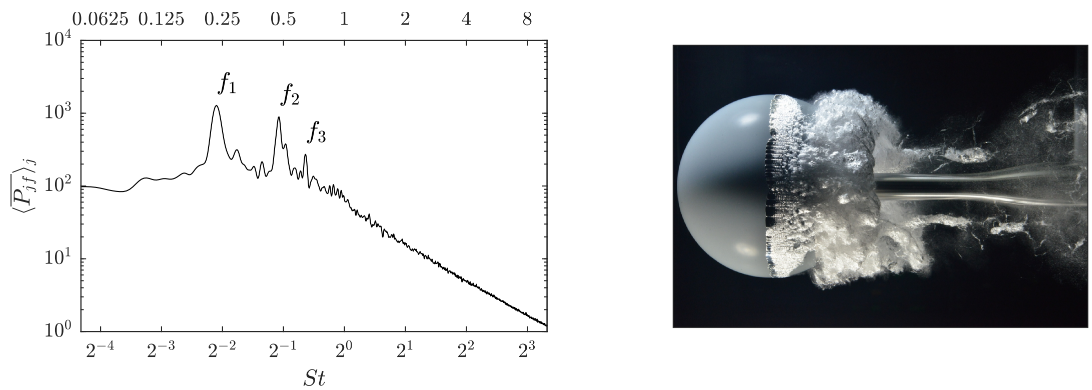

Figure 1: Spatial average (left) of all spectra across the domain identifying three peaks. Photograph (right) showing typical flow state at a cavitation number of 0.8.

It is less straightforward to produce a representative view of the phase angle, however, since it is constantly changing and thus a temporal average of ϕ_{jtf} will not be meaningful. In fact, given enough t instances, the temporal average will be zero. The phase of different windows are given in figure 2. The same general flow pattern can be seen in each, though the phase is offset by some angle between the instances. The phase offset is approximately the ratio of the time shift (N_S) to the temporal wavelength of the structure. To present an 'averaged' view of the phase information from each of the windows, the singular value decomposition (SVD) was used to decompose the Fourier coefficients and return a series of SVD-modes, the first being most representative of the spatial mode corresponding to each frequency. The matrix $\boldsymbol{\Phi}_f$ is constructed in which each column represents a different window (t) of the phase of one frequency – the size of this matrix is $J \times T$ (for the present study: $2^{19} \times 51$):

$$
\begin{array}{cc}
 & \xrightarrow{\quad \text{Welch windows} \quad} \\
\boldsymbol{\Phi}_f = & \begin{bmatrix}
X_{j=1,t=1} & X_{j=1,t=2} & \dots & X_{j=1,t=T} \\
X_{j=2,t=1} & X_{j=2,t=2} & \dots & X_{j=2,t=T} \\
\vdots & \vdots & \ddots & \vdots \\
X_{j=J,t=1} & X_{j=J,t=2} & \dots & X_{j=J,t=T}
\end{bmatrix} \Big\downarrow \text{Spatial domain}
\end{array}
\tag{3}
$$

The SVD factorizes the complex field $\boldsymbol{\Phi}_f$, decomposing it with:

$$
\boldsymbol{\Phi}_f = \boldsymbol{L_f \Sigma_f R_f} \tag{4}
$$

Which returns $\boldsymbol{L}_f$: a series of orthonormal eigenvectors of $\boldsymbol{\Phi}_f \boldsymbol{\Phi}_f^T$ which is a square matrix of size $J \times J$, $\boldsymbol{\Sigma}_f$: a rectangular matrix where the diagonal contains T values that are the square-root of the eigenvalues (these correspond to how much of the variability in $\boldsymbol{\Phi}_f$ is accounted for in each SVD-mode), and $\boldsymbol{R}_f$: a series of eigenvectors of $\boldsymbol{\Phi}_f^T \boldsymbol{\Phi}_f$; a square matrix of size $T \times T$.

*Corresponding Author, James Venning: mail@jamesvenning.net

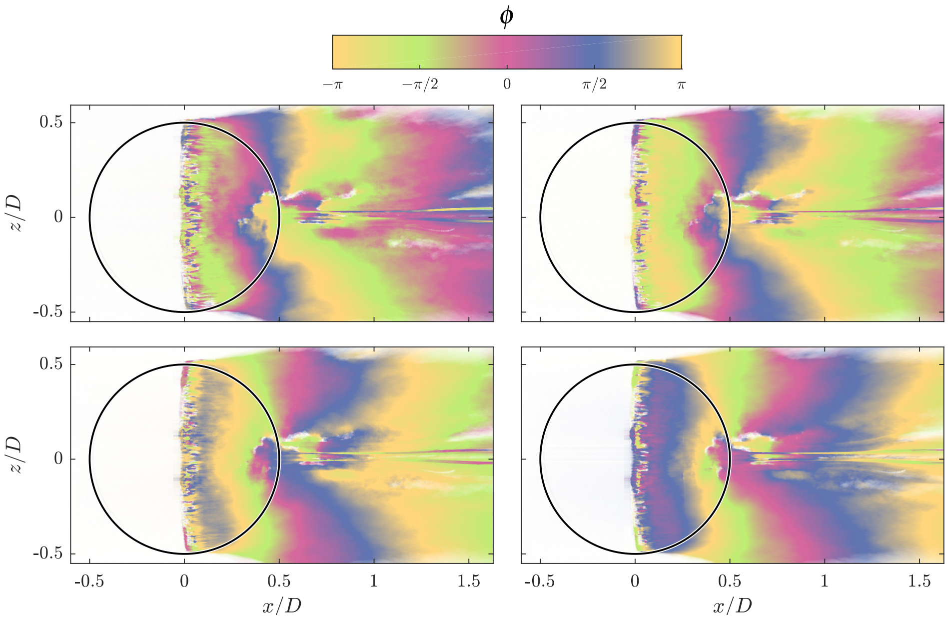

Figure 2: Phase angle of the fundamental cavitation shedding frequency about a sphere at $\sigma = 0.8$. Sequential instances of time (Welch windows) are displayed.

The T SVD-modes are the projections of $\boldsymbol{\Phi}_f$ onto the basis eigenvectors ($\boldsymbol{\Phi_f R_f}$). This mode shape and the corresponding variance (from $\boldsymbol{\Sigma}_f$) of each SVD-mode for the second frequency (f_2 from figure 1) are given in figure 3. The first SVD-mode captures the bulk of the variance, so should be the most representative of the phase field. This is verified by comparing figure 2 with figure 3, and as such it is the only SVD-mode presented for the remainder of the paper. The most useful result of the modal analysis is the spatial phase information of each frequency across the video frame revealing the direction of the cavity flow, and more importantly the regions of the flow that are travelling in phase.

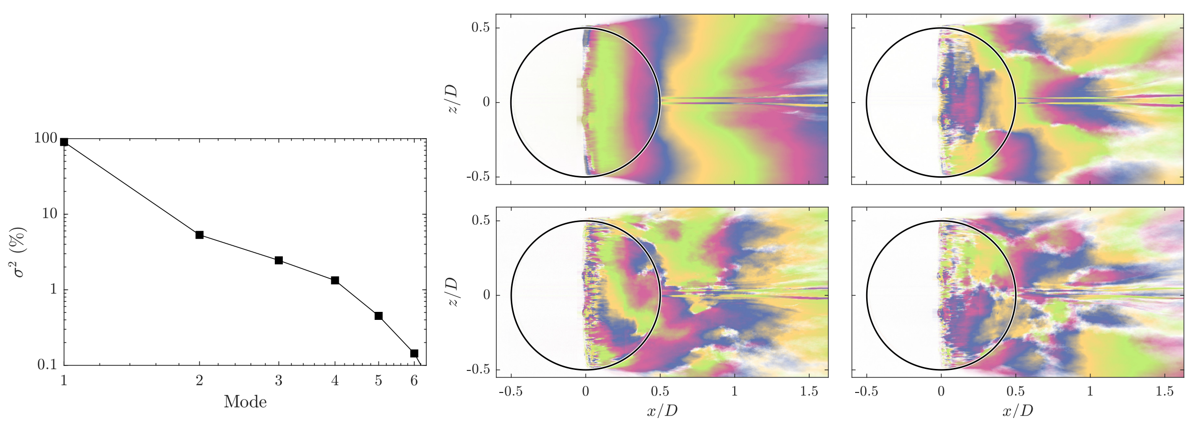

Figure 3: Variance (top) of each of the f_2 SVD-modes (bottom) as a percentage of the total variance. The first SVD-mode contributes 90.3% of the total variance, representing the most likely phase pattern in the flow, and corresponds well to the instantaneous frames in figure 2. The mode number increases across the page first.

The first SVD-mode for each of the three shedding frequencies from figure 1 are presented in figure 4. The primary large-scale shedding mode is $f_2 = 0.48$. In this mode, the cavity is shed as a series of ring-like vortices that become oblique in the wake (figure 5). Visualisation of this shedding mode suggests that it is quite powerful for most of the wake portion captured by the video frame, particularly for $0.2 < x/D < 0.7$. The mode is symmetric about the $z/D = 0$ plane, reminiscent of the ring-like vortices from a shedding sphere at $300 < Re < 420$ presented in [9]. The shed cavities condense near $x/D = 0.8$, which is why the energy content decays from then on.

*Corresponding Author, James Venning: mail@jamesvenning.net

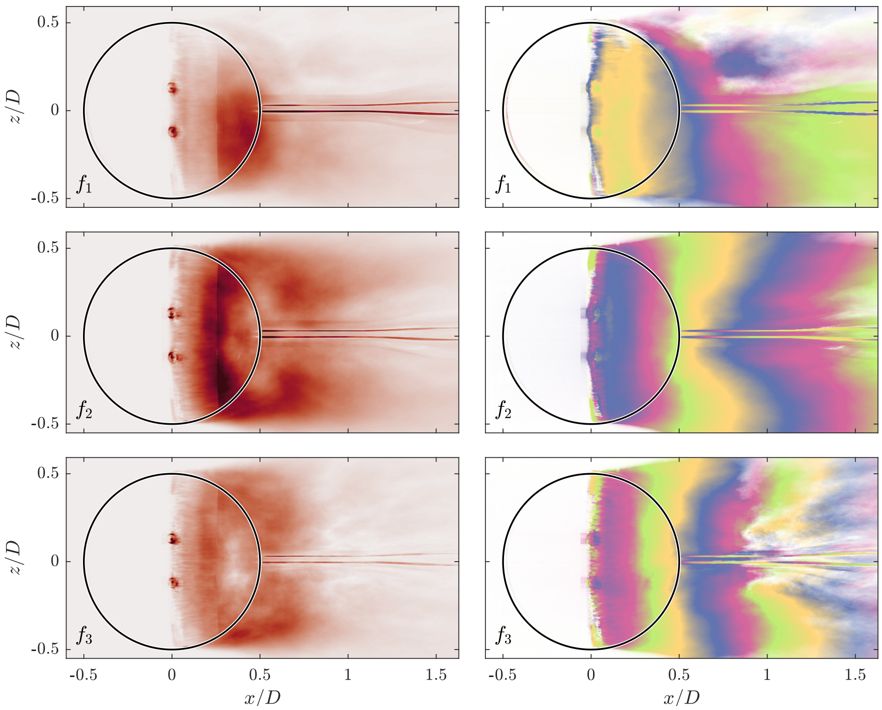

Figure 4: Frequency information for the flow around a sphere at $\sigma = 0.8$. The left hand column contains the spatial distribution of the power, and the right-hand column is the phase of those structures. The mode power is normalised to the maximum power of that frequency.

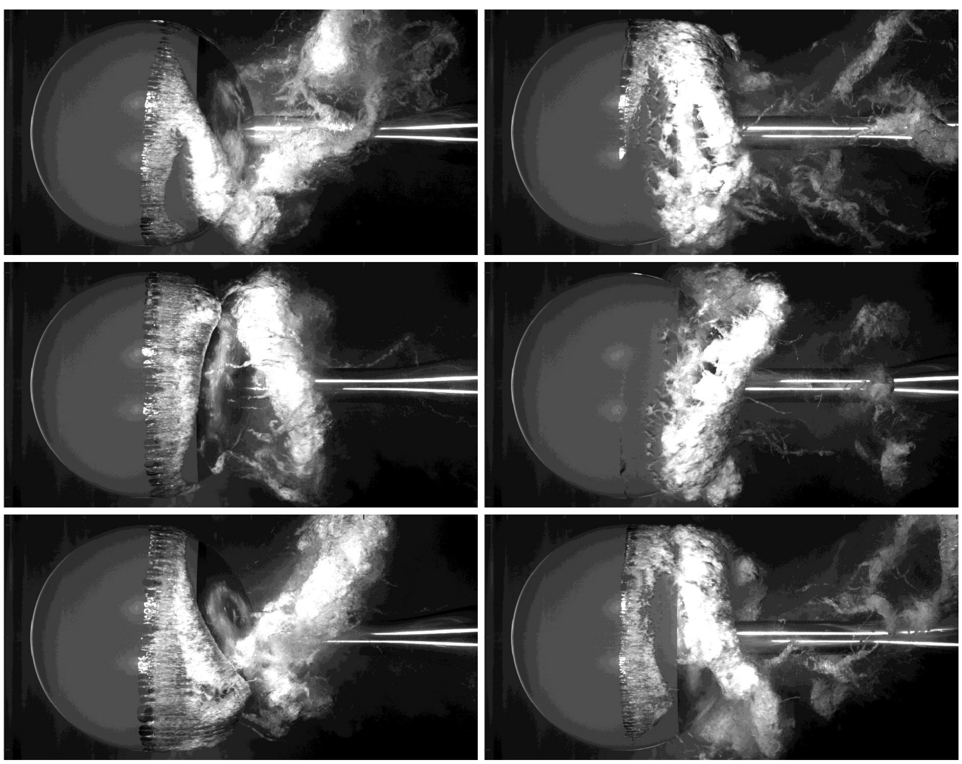

Figure 5: Six equi-spaced photographs capturing three cycles of the f_2 shedding mode, showing alternating oblique vortex shedding. The images are separated by half the period, such that each column is at a single phase.

One difficulty with this technique is that the phase information is averaged over the window of interest, so when different flow features occur at the same frequency, the results are misleading. For example, examining the high-

*Corresponding Author, James Venning: mail@jamesvenning.net

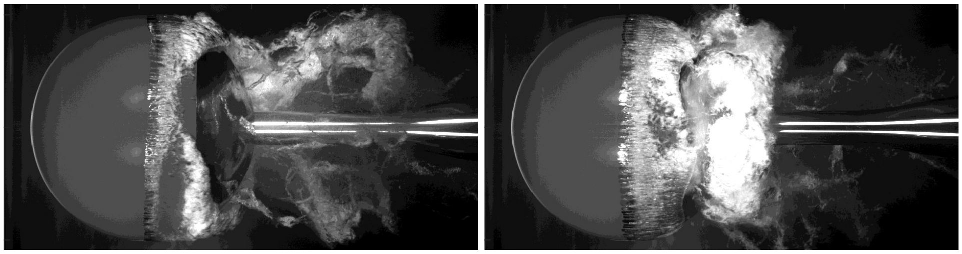

Figure 6: Photographs showing a single cycle of the f_1 shedding frequency. The images are separated by half the period.

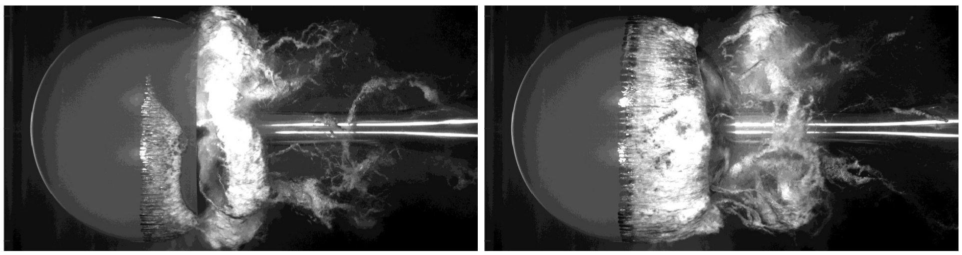

Figure 7: Photographs showing a single cycle of the f_3 shedding frequency. The images are separated by half the period.

speed footage in regions where the f_2 peak is powerful (figure 5) suggests that the shed vortices are actually oblique, alternating slope with each cycle. So, while the average of the phase is, in-fact, symmetrical, the individual structures may be oblique, thus care must be taken to investigate the original videos to understand the true nature of the modes. A clue to the true shape of this mode may be in the second of the SVD modes presented in figure 3, which shows oblique structures. Additionally, considering only one half ($z/D > 0$) of the phase diagram in figure 4 shows the angled nature of the shedding.

The first shedding mode, $f_1 = 0.23$ is concentrated in the near-wake of the sphere (figure 6). It is a sub-harmonic of the primary frequency. It is slightly more dominant in the bottom than the top, suggesting that this mode could be suppressed to some extent by the sting and/or hydrostatic differences. The shed cavities often take the appearance of hair-pin vortices (figure 6).

A third shedding mode, $f_3 = 0.64$, is also symmetric. Analysis of the video (figure 7) suggests that this frequency is associated with a very short cavity followed by a longer cavity. The initial cavity is still in the near vicinity of the body when the second cavity is growing. The energy of this higher frequency mode dissipates earlier than f_2, with this short cavity being replaced by one of the two large-scale events.

Conclusion

A technique for decomposing time-resolved visual data is presented using a Fourier transform to determine the spatial distribution of power for all frequencies of interest. The resulting reconstructed images reveal the locations within the image that experience a given frequency.

The structure of the phase can be determined by a singular value decomposition of the different phase windows. The phase information is useful to show the nature of the oscillations, but care must be taken that the spatial mode is, in fact, exemplary of the actual flow structures.

We use a high-speed video of cavitation about a sphere to show how this technique can be used to aid in the understanding of the mechanisms associated with the three shedding frequencies of interest. The main shedding mode was shown to be due to the shedding of large, oblique cavitation clouds, alternating in gradient in successive cycles. The subharmonic mode was related to symmetric, large-scale cavitation, while the harmonic mode was single-event, short-duration, cavities.

*Corresponding Author, James Venning: mail@jamesvenning.net

References

[1] Lawrence Sirovich. *Turbulence and the dynamics of coherent structures.* Quarterly of Applied Mathematics, 45 (3), 1987. ISSN 0033-569X. doi: 10.1090/qam/910463.

[2] Clarence W. Rowley, Igor Mezić, Shervin Bagheri, Philipp Schlatter, and Dan S. Henningson. *Spectral analysis of nonlinear flows*. Journal of Fluid Mechanics, 641, 2009. ISSN 0022-1120. doi: 10.1017/S0022112009992059.

[3] Peter J. Schmid. *Dynamic mode decomposition of numerical and experimental data*. Journal of Fluid Mechanics, 656, 2010. ISSN 0022-1120. doi: 10.1017/S0022112010001217.

[4] J. Basley, L. R. Pastur, F. Lusseyran, T. M. Faure, and N. Delprat. *Experimental investigation of global structures in an incompressible cavity flow using time-resolved PIV*. Experiments in Fluids, 50(4), 2011. ISSN 07234864. doi: 10.1007/s00348-010-0942-9.

[5] J. Basley, L. R. Pastur, N. Delprat, and F. Lusseyran. *Space-time aspects of a three-dimensional multi-modulated open cavity flow*. Physics of Fluids, 25(6), 2013. ISSN 10706631. doi: 10.1063/1.4811692.

[6] T. Mcqueen, J. Venning, and J. Sheridan. Effects of Aspect Ratio on the Wake Dynamics of the Ahmed Body. In *19th Australasian Fluid Mechanics Conference*, 2014. ISBN 9780646596952.

[7] J Venning. *Vortex structures in the wakes of two- and three-dimensional bodies*. Phd, Monash University, 2016.

[8] K. L. de Graaf, P. A. Brandner, and B. W. Pearce. *Spectral content of cloud cavitation about a sphere*. Journal of Fluid Mechanics, 812, 2017. ISSN 0022-1120. doi: 10.1017/jfm.2016.819.

[9] H Sakamoto and H Haniu. *A Study on Vortex Shedding From Spheres in a Uniform Flow*. Transactions of the ASME Journal of Fluids Engineering, 112, 1990.

*Corresponding Author, James Venning: mail@jamesvenning.net